



## Rapid Communication

# Polymer Core-Polymer Shell Particle Formation Enabled by Ultralow Interfacial Tension Via Internal Phase Separation: Morphology Prediction Using the Van Oss Formalism



Markus Andersson Trojer<sup>a,b,\*</sup>, Anna Ananievskaia<sup>c</sup>, Asvad A. Gabul-Zada<sup>c</sup>, Lars Nordstierna<sup>d</sup>, Hans Blanck<sup>c</sup>

<sup>a</sup> Department of Colloid Chemistry, Max Planck Institute of Colloids and Interfaces, Potsdam, Germany

<sup>b</sup> Department of Materials, Bio-based fibres, Swerea IVF, Mölndal, Sweden

<sup>c</sup> Department of Biological and Environmental Sciences, University of Gothenburg, Göteborg, Sweden

<sup>d</sup> Department of Chemistry and Chemical Engineering, Chalmers University of Technology, Göteborg, Sweden

## ARTICLE INFO

## Keywords:

Microcapsule  
Solvent evaporation  
Core-shell  
Raspberry  
Janus  
Spreading

## ABSTRACT

The internal phase separation technique is a versatile method for liquid core-polymer shell formation, yet limited to very hydrophobic core materials and actives. The use of polymeric cores instead circumvents this restriction due to the absent mixing entropy for binary polymer mixtures which allows the polymeric core (and the active) to approach the polarity of the shell. Polystyrene core-shell and janus particles were formulated using polymethylmethacrylate, poly(lactic acid), poly(lactic acid-co-glycolic acid), poly( $\epsilon$ -caprolactone) or cellulose triacetate as shell-forming polymers. The morphology and the partitioning was experimentally determined by selectively staining the core and the shell with  $\beta$ -carotene and methylene blue respectively. In addition, the van Oss formalism was introduced to theoretically predict the thermodynamic equilibrium morphology. As elucidated using the theoretical predictions as well as experimental optical tensiometry, it was found that the driving force for core-shell morphology is, in contrast to liquid core-polymer shell particles, a low core-shell interfacial tension.

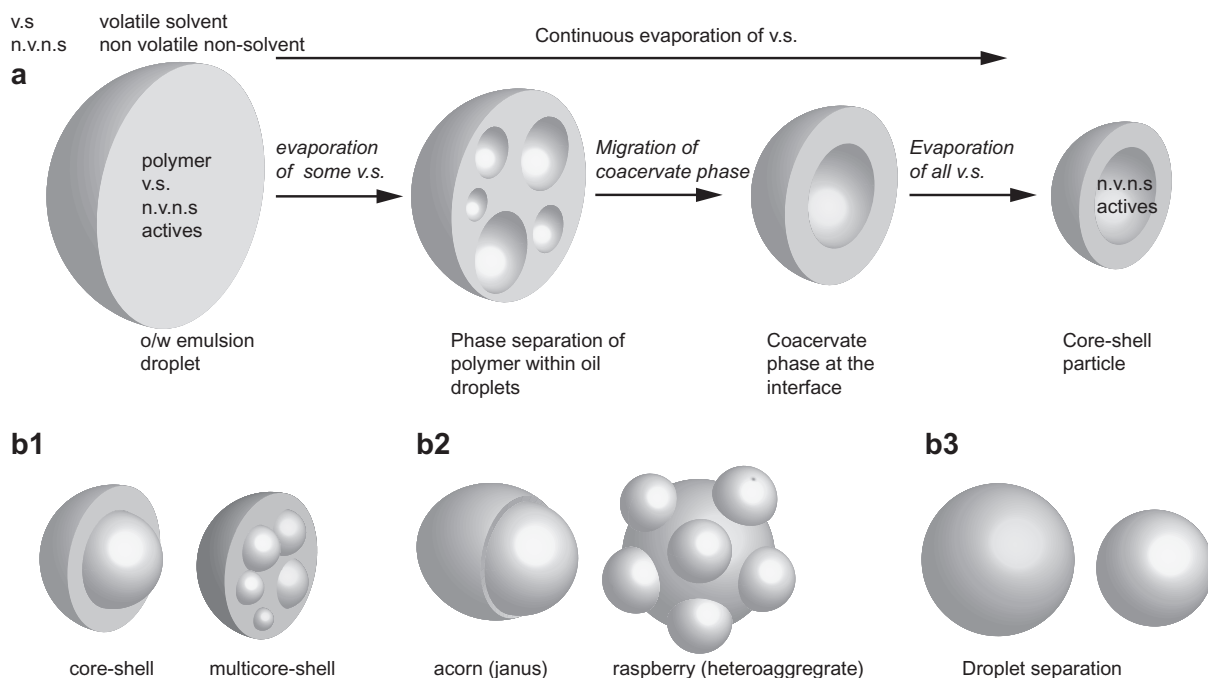
Microencapsulation is an important technology for the protection and/or controlled release of active substances [1–4]. Among the available encapsulation methods, the internal phase separation route [5] has increased in popularity during the last decade [1]. This popularity can be ascribed to its versatility in terms of possible shell (usually polymeric) and core material (usually a liquid), encapsulation efficiencies often approaching 100%, absence of residual reactive species (e.g. monomers or initiators used for interfacial polymerization encapsulation), good control over core and shell dimensions and to its feasibility for industrial scale-up [1]. The theoretical basis and experimental details of the method are discussed on the next page. Most often, the microcapsules comprise liquid cores which may give a faster release than intended due to the high diffusivity of the actives in liquids. This can be circumvented by using alkanes which are solid at room temperatures and by performing the encapsulation at slightly elevated temperatures above their melting temperatures [6]. Another issue with liquid cores is the restriction in terms of their polarity imposed by the spreading requirements of the internal phase separation method [1,5]. This restriction is discussed in detail below. In short, for encapsulation

in aqueous media, the core engulfment by the polymeric shell necessitates that the core liquid is sufficiently hydrophobic (e.g. alkanes) [5,7]. This has consequences for moderately hydrophobic actives which, more than occasionally, prefer the shell rather than the core [8].

The use of polymeric cores instead of liquid ones will obviously influence the release rate since the diffusion coefficient of actives in the core will be reduced by orders of magnitude [1]. Yet, more importantly, polymeric cores are allowed to be much more polar than their liquid counterparts, approaching the polarity of the polymeric shell. This is a consequence of the absent mixing entropy for binary polymer mixtures which enables polymers of similar polarity to remain immiscible. Subsequently, a wider range of more polar actives may be encapsulated by using polymeric cores.

In this report, formation of core-shell particles comprising a polystyrene core and various polymeric shells is presented. Dyes of different polarities have been used to selectively envisage the core and shell respectively. In addition, the van Oss formalism is presented as a tool to predict the microcapsule morphology and to determine whether encapsulation is theoretically conceivable or not for a given core-shell

\* Corresponding author at: Swerea IVF, Department of materials, Division of bio-based fibers, Argongatan 30, 431 53 Mölndal, Sweden.  
E-mail address: [markus.andersson-trojer@swerea.se](mailto:markus.andersson-trojer@swerea.se) (M. Andersson Trojer).



**Scheme 1.** a) Encapsulation process via the internal phase separation route. b) Possible morphologies and outcomes of the microencapsulation: b1) core-shell, b2) acorn-shaped morphology, and b3) droplet separation. The most common system, used for encapsulation of hydrophobic dyes, is an O/W emulsion. The aqueous phase contains a dispersant (typically a water-soluble polymer such as PVA) and the oil phase contains a volatile solvent (v.s.), the shell-forming polymer, the core material (usually an oil which is a non-solvent for the polymer, n.v.n.s) [1,6] (see Chart 1).

pair.

Encapsulation based on internal phase separation relies on the internal segregation and subsequent spreading of coacervate phases inside an emulsion droplet (see Scheme 1a). The means for phase separation is the continuous evaporation of the v.s. which subsequently leads to phase segregation as the ternary composition reaches the binodal curve of the phase diagram and eventually to solidification. An oil which is too polar will either remain miscible with the polymer (see Chart 1) or prevent polymer spreading as discussed below.

For microencapsulation and core-shell formation, it is necessary that the shell polymer (assigned S) wets the core material (usually an oil or as in this report, a polymer, assigned C) and the aqueous phase

(assigned W) (see Scheme 1). The spreading coefficient  $S_S$  is defined by the free energy for cohesion  $\Delta G_S^c$  and adsorption  $\Delta G_S^a$  in Eq. (1) as;

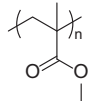
$$S_S = \Delta G_S^c - \Delta G_S^a = \gamma_{C/W} - (\gamma_{S/W} + \gamma_{C/S}) \quad (1)$$

The spreading coefficients were used by Torza and Mazon [9] to determine the morphology of a system comprising three immiscible liquids. The theory was later used to encompass phase segregating polymers [5,7,10]. Assuming that  $\gamma_{C/W} > \gamma_{C/S}$ , three possible sets of spreading conditions are obtained (Eqs. (2)–(4)) [5,9];

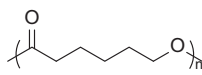
$$S_C < 0; \quad S_W < 0; \quad S_S > 0 \quad (2)$$

$$S_C < 0; \quad S_W < 0; \quad S_S < 0 \quad (3)$$

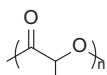
## Shell polymers



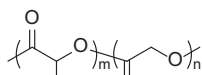
**PMMA**  $\delta$ : 19.0  
Poly(methyl methacrylate)



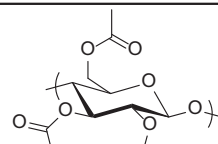
**PCL**  $\delta$ : 19.1  
Poly(ε-caprolactone)



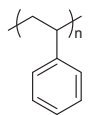
**PLLA**  $\delta$ : 21.0  
Poly(L-lactic acid)



**PLGA**  $\delta$ : 22.3 (m/n≈1)  
Poly(lactic acid-co-glycolic acid)



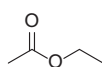
**CTA**  $\delta$ : 21.2  
Cellulose triacetate



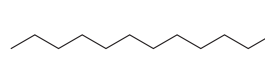
$\delta$ : 18.7  
n.v.n.s.  
**PS**  
Polystyrene



$\delta$ : 18.7  
v.s.  
**Chloroform**

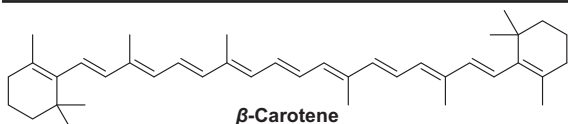


$\delta$ : 18.7  
v.s.  
**Ethyl acetate**

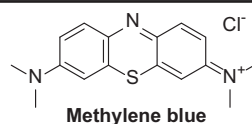


$\delta$ : 16.0  
n.v.n.s.  
**Dodecane**

## Core polymer and liquids



$\log K_{ow}$ : 15.51  
 $\delta$ : 12.3



$\log K_{ow}$ : 2.61

## Dyes

**Chart 1.** Polymers used for shells, oils/polymers used for cores and dyes used for encapsulation. Solubility parameters ( $\delta$ [MPa<sup>1/2</sup>]) and the logarithm of the octanol-water partition coefficient ( $\log K_{ow}$ ) are provided, as obtained from chemical databases (see the Supplementary Material, Table S1).

$$S_C < 0; \quad S_W > 0; \quad S_S < 0 \quad (4)$$

The core-shell morphology can only be obtained if the conditions in Eq. (2) are satisfied. Eq. (3) will generate so-called *acorn particles* and Eq. (4) will result in separate oil and polymer droplets [1,5,7]. It is clear that the core-shell formation requires that  $\gamma_{C/W}$  remains high.

To experimentally determine the spreading coefficients is rather time-consuming if the intention is only to find a suitable core-shell pair. In addition, to experimentally measure the interfacial tension between polymers is difficult and usually performed on melts [11]. Instead, the morphology can be predicted by theoretically calculating the interfacial tensions.

We have found that the van Oss-Chaudhury-Good formalism (Eqs. (5)–(8)) [12,13], which takes asymmetric Lewis acid-base interactions into account, provides an adequate compromise between accuracy and simplicity. The apolar  $\gamma_i^{LW}$  contribution is expressed as the total Lifshitz, or van der Waals, force and the polar term  $\gamma_i^{AB}$  accounts only for Lewis acid-base interaction. The polar term is expressed by an acid component  $\gamma_i^+$  and a base component  $\gamma_i^-$  (see Eq. (6)) [12].

$$\gamma_i = \gamma_i^{LW} + \gamma_i^{AB} \quad (5)$$

$$\gamma_i^{AB} = 2\sqrt{\gamma_i^+ \gamma_i^-} \quad (6)$$

The interfacial tension components may now be expressed by the geometric mean and the surface energy components for polymers can be found in proper databases (see Supplementary Material).

$$\gamma_{ij}^{LW} = (\sqrt{\gamma_i^{LW}} - \sqrt{\gamma_j^{LW}})^2 \quad (7)$$

$$\gamma_{ij}^{AB} = 2(\sqrt{\gamma_i^+} - \sqrt{\gamma_j^+})(\sqrt{\gamma_i^-} - \sqrt{\gamma_j^-}) \quad (8)$$

In short, the core-shell or janus particles were prepared by dissolving PS, the shell polymer of choice (Chart 1) and dyes in the v.s. dichloromethane (containing small amounts of acetone depending on the shell polymer, see the Supplementary Material). The oil phase was subsequently emulsified in 1 wt% PVA aqueous solution and the emulsion was allowed to transform into a polymeric suspension at ambient conditions via evaporation of the v.s. for 24 h. The resulting core-shell or janus particles were analysed using bright field microscopy (Olympus BH-2 equipped with a digital camera Olympus DPI, Olympus Sverige, Solna, SE). The interfacial and surface free energy of the liquids and smooth nanometre thick polymers films spin-coated on quartz crystals (see the Supplementary Material) were determined using optical tensiometry (Theta optical tensiometer, Attension, Espoo, FI).

The van Oss formalism predicts core-shell morphology as seen in Table 1 for all systems investigated. This is to a large extent due to the ultralow polystyrene-polymer interfacial tension ( $\gamma_{C/S}$ , see the Supplementary Material, Table S2). This is in sharp contrast to the core-shell formation for liquid core-polymer-shell formation. For these systems, the driving force is a high core-water interfacial tension as mentioned

**Table 1**

Theoretically and experimentally calculated spreading coefficients for PS cores with various polymer shells.

Shell	$S_C$	$S_S$	$S_W$	Morphology	
				Predicted	Observed
PMMA	-5.1	3.4	-72.3	Core-shell	Core-shell
PMMA <sup>a</sup> (exp)	-5.1	5.0	-42.6	Core-shell	Core-shell
PMMA <sup>b</sup> (exp)	-5.1	5.0	-42.8	Core-shell	Core-shell
PLLA	-25.4	18.8	-52.0	Core-shell	Raspberry
PLGA	-29.3	25.9	-58.1	Core-shell	Core-shell
PCL	-23.7	18.8	-53.8	Core-shell	Acorn
PCL <sup>a</sup> (exp)	-13.9	-1.3	-33.7	Acorn	Acorn
CTA	-35.0	33.7	-42.5	Core-shell	Core-shell

<sup>a</sup>Based on experimentally measured interfacial tensions using polyvinylalcohol or polymethacrylic acid<sup>b</sup> as aqueous emulsifiers.

above which prevents the use of surfactants as dispersants. The prediction is correct for all systems except for the aliphatic polyesters poly(L-lactic acid) (PLLA) and poly( $\epsilon$ -caprolactone) (PCL) (see Table 1 and Fig. 1). The deviation in terms of the sign of  $S_S$  for the PCL-based system is discussed in detail in the Supplementary Material. The PS-PLLA particles displayed raspberry-type (heteroaggregate) morphology whereas the PS-PCL particles were perfect acorn-type janus particles. This result does not seem to correlate with the magnitude of any of the three spreading coefficients. As an example, multicore morphology has previously been correlated with the magnitude of  $S_S$ . However, it is important to realize that the van-Oss prediction does not take dispersant or kinetic effects into account and should consequently be implemented to determine whether encapsulation is theoretically possible or not for a given system.

In one of the few earlier studies of polymer core-polymer shell particles, focusing on much larger capsules ( $\sim$ mm-sized), Pekarek et al. also obtained heteroaggregates for the PS-PLLA system [10]. The authors speculated that it should be possible to trap core-shell morphology given that the initial phase separated coacervate morphology is core-shell. The use of coacervate phases for determination of the spreading conditions has been used by others to successfully predict the microcapsule morphology [7]. However, the literature is inconsistent with respect to the morphology outcome based on kinetic entrapment or slow phase segregation approaching thermodynamic equilibrium. Both formation of core-shell and acorn particles at slow and fast solvent evaporation [14,15] respectively and vice versa [16] have been reported. However, we believe that it is inconceivable to predict a pre-disposition for core-shell morphology based on the coacervate phases during the course of the phase separation. Especially since  $S_S$  starts at zero and approaches the asymptotic phase-separated value during the course of the internal phase separation (see the Supplementary Material). Instead, it is only conceivable to obtain metastable morphologies other than core-shell over a narrow initial concentration interval for polymer shells for which  $\gamma_{S/W} > \gamma_{v.s./W}$  and for which the v.s. has a strong segregation towards the core polymer (see the Supplementary Material, Figs. S7 and S8).

For the systems investigated in this report, the opposite behavior is observed, i.e. the polyesters for which  $\gamma_{S/W} < \gamma_{v.s./W}$  (see the Supplementary Material, Table S2 and Fig. S8) displayed acorn morphologies, albeit at various incidence. The observed morphologies for the polyesters can consequently not be explained by thermodynamic arguments. It is plausible that a dominating kinetic contribution to the morphology outcome is a generic feature for polymeric binary encapsulation systems. Engulfment and spreading is most likely hindered by the immobile viscous concentrated polymer coacervate phases. This hypothesis would explain the morphological discrepancy observed for the aliphatic polyesters. Both PCL and PLLA displayed the highest theoretical and experimental  $\gamma_{C/S}$  values (see the Supplementary Material, Table S2) and consequently the highest phase incompatibility. This could indicate a lower tendency for coacervate spreading as the oil droplet phase separates into a PS- and a polyester-rich phase. It should be noted that a small fraction of the aforementioned particle systems displayed core-shell morphology corroborating the kinetic nature of this particular morphology outcome.

The purpose of using dyes has in this study been twofold. By choosing dyes of a given polarity (as determined by e.g.  $\log K_{ow}$  or  $\delta$ , see Chart 1), the partitioning of actives of similar polarities can qualitatively be determined. In a similar manner, by choosing dyes with different partitioning propensities, the morphology of a given polymer core-polymer shell system can be visualized. In Fig. 1a, PS-core PMMA-shell capsules have been stained with  $\beta$ -carotene and methylene blue.  $\beta$ -carotene was chosen due to its hydrophobicity and the semihydrophobic methylene blue due to its relatively high polarity (see Chart 1). As can be seen in the inset a1 in Fig. 1,  $\beta$ -carotene has clearly partitioned into the hydrophobic PS core whereas methylene blue prefers the semihydrophobic PMMA shell.

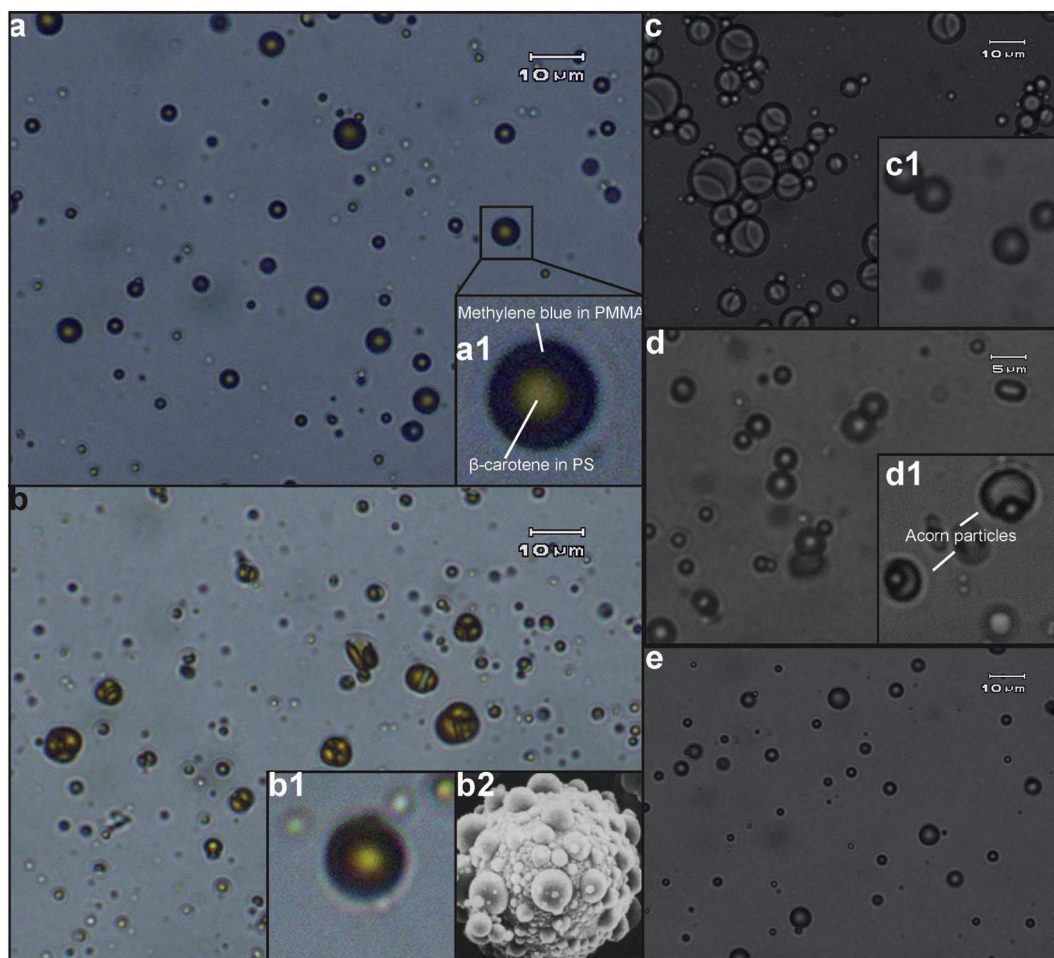


**Fig. 1.** a) PS-core PMMA-shell capsules stained with  $\beta$ -carotene and methylene blue. The inset (a1) displays a close-up on the PMMA shell coloured blue using methylene blue and the PS core coloured yellow using  $\beta$ -carotene. b) Raspberry-type (heteroaggregates) PS-PLLA particles dyed yellow using  $\beta$ -carotene. The inset (b1) displays a close up on one of the rare examples of PS-core PLLA-shell particles. As can be seen,  $\beta$ -carotene has to a larger extent partitioned into the PS core. The inset (b2) displays a SEM image of a mm-sized heteroaggregate PS-PLLA particle obtained by Pekarek et al. (Reprinted by permission from Macmillan Publishers Ltd: Nature: 367, 258–260, ©1994) [10]. c) Acorn janus particles consisting of PCL partially engulfing PS. Note that also this polymer combination sporadically displayed core-shell particles (c1). d) PS-core PLGA-shell particles. The occurrence of acorn particles (d1) was for this polymer combination less frequent. e) PS-core CTA-shell particles. (For interpretation of the references to colour in this figure legend, the reader is referred to the web version of this article.)

In conclusion, polymer core-polymer shell particles consisting of a polystyrene core and various polymer types as shells have been formulated by internal phase separation in O/W emulsions. Using polymer cores instead of liquid ones enables much more polar cores to be encapsulated. Theoretical calculations of the spreading coefficients using the van-Oss formalism has been successfully introduced to predict the morphology outcome of the internal phase separation. Most polymer pairs gave core-shell morphology as predicted. However, the PS-PCL pair gave janus particles and the PS-PLLA pair gave heteroaggregates, most likely due to kinetic factors mediated by a relatively high phase incompatibility. Yet, the generic propensity for core-shell morphology is primarily a consequence of the very low  $\gamma_{C/S}$  interfacial tension which is supported by both kinetic and thermodynamic arguments. For particles formulated using the polymer pair PS-PMMA, the core and the shell were selectively stained using  $\beta$ -carotene and methylene blue respectively.

#### Declaration of Interest

None.

#### Acknowledgement

The Swedish Research Council FORMAS (2012-86 and 2016-61), Vinnova (2017-04693) and the foundation *Bengt Lundqvist minne* (post-doctoral grant, no grant number available) are acknowledged for funding.

#### Appendix A. Supplementary data

Supplementary data to this article can be found online at <https://doi.org/10.1016/j.colcom.2018.07.001>.

#### References

- [1] M. Andersson Trojer, Polymeric core-shell particles: physicochemical properties and controlled release, in: P. Somasundaran (Ed.), *Encyclopedia of Surface and Colloid Science*, Taylor and Francis, New York, 2015, <http://dx.doi.org/10.1081/E-ESCS-120048578>.
- [2] M. Andersson Trojer, L. Nordstierna, M. Nordin, B.M. Nyden, K. Holmberg, Encapsulation of actives for sustained release, *Phys. Chem. Chem. Phys.* 15 (41) (2013) 17727–17741, <http://dx.doi.org/10.1039/C3CP52686K>.
- [3] H.N. Yow, A.F. Routh, Formation of liquid core-polymer shell microcapsules, *Soft Matter* 2 (11) (2006) 940–949.
- [4] M. Andersson Trojer, Y. Li, C. Abrahamsson, A. Mohamed, J. Eastoe, K. Holmberg, M. Nyden, Charged microcapsules for controlled release of hydrophobic actives part I: encapsulation methodology and interfacial properties, *Soft Matter* 9 (5) (2013)

- 1468–1477, <http://dx.doi.org/10.1039/C2SM27275J>.
- [5] A. Loxley, B. Vincent, Preparation of poly(methyl methacrylate) microcapsules with liquid cores, *J. Colloid Interface Sci.* 208 (1) (1998) 49–62, <http://dx.doi.org/10.1006/jcis.1998.5698>.
- [6] M. Andersson Trojer, L. Nordstierna, J. Bergek, K. Holmberg, B.M. Nyden, Use of microcapsules as controlled release devices for coatings, *Adv. Colloid Interf. Sci.* 222 (2015) 18–43.
- [7] A.L. Tasker, J.P. Hitchcock, L. He, E.A. Baxter, S. Biggs, O.J. Cayre, The effect of surfactant chain length on the morphology of poly(methyl methacrylate) microcapsules for fragrance oil encapsulation, *J. Colloid Interface Sci.* 484 (2016) 10–16, <http://dx.doi.org/10.1016/j.jcis.2016.08.058>.
- [8] A. Enejder, F. Svedberg, L. Nordstierna, M. Nyden, Chemical release from single-PMMA microparticles monitored by CARS microscopy, *Proc. SPIE* 7903 (2011) (79030S/1-79030S/8), <https://doi.org/10.1117/12.874537>.
- [9] S. Torza, S.G. Mason, Three-phase interactions in shear and electrical fields, *J. Colloid Interface Sci.* 33 (1) (1970) 67–83, [http://dx.doi.org/10.1016/0021-9797\(70\)90073-1](http://dx.doi.org/10.1016/0021-9797(70)90073-1).
- [10] K.J. Pekarek, J.S. Jacob, E. Mathiowitz, Double-walled polymer microspheres for controlled drug release, *Nature (London)* 367 (6460) (1994) 258–260, <http://dx.doi.org/10.1038/367258a0>.
- [11] G. Biresaw, C.J. Carriere, Interfacial tension of poly(lactic acid)/polystyrene blends, *J. Polym. Sci. B Polym. Phys.* 40 (19) (2002) 2248–2258, <http://dx.doi.org/10.1002/polb.10290>.
- [12] R.J. Good, C.J. Van Oss, The modern theory of contact angles and the hydrogen bond components of surface energies, in: M.E. Schrader, G.I. Loeb (Eds.), *Mod. Approaches Wettability*, Plenum Press, New York, 1992, pp. 1–27.
- [13] C.J. Van Oss, R.J. Good, M.K. Chaudhury, Additive and nonadditive surface tension components and the interpretation of contact angles, *Langmuir* 4 (4) (1988) 884–891, <http://dx.doi.org/10.1021/la00082a018>.
- [14] P.J. Dowding, R. Atkin, B. Vincent, P. Bouillot, Oil core-polymer shell microcapsules prepared by internal phase separation from emulsion droplets. I. Characterization and release rates for microcapsules with polystyrene shells, *Langmuir* 20 (26) (2004) 11374–11379, <http://dx.doi.org/10.1021/la048561h>.
- [15] R. Atkin, P. Davies, J. Hardy, B. Vincent, Preparation of aqueous core/polymer shell microcapsules by internal phase separation, *Macromolecules* 37 (21) (2004) 7979–7985.
- [16] S. Tang, M. Yourdkhani, C.M. Possanza Casey, N.R. Sottos, S.R. White, J.S. Moore, Low-ceiling-temperature polymer microcapsules with hydrophobic payloads via rapid emulsion-solvent evaporation, *ACS Appl. Mater. Interfaces* (2017), <http://dx.doi.org/10.1021/acsami.7b05266>.